

# RadLib: a radiative property model library for CFD

Victoria B. Stephens, Sally Jensen, Isaac Wheeler, David O. Lignell\*

*Department of Chemical Engineering, Brigham Young University, Provo, UT 84602,  
United States*

---

## Abstract

RadLib is a C++ library of radiation property models that can be applied to variety of systems involving radiative heat transfer, including CFD simulations. RadLib includes three major radiation property models—Planck Mean (PM) absorption coefficients, the weighted sum of gray gases (WSGG) model, and the rank-correlation spectral line weighted-sum-of-gray-gases (RCSLW) model. RadLib includes C++, Python, and Fortran interfaces and can be expanded to include additional models. Several example cases illustrate use of the models with an included ray-tracing solver, compare their accuracy relative to line-by-line (LBL) solutions, and examine their computational costs. Additionally, an integrated CFD example of an ethylene burner configuration using Fire Dynamics Simulator (FDS) is provided. RadLib provides researchers with convenient access to validated radiation property models and a framework for further development.

*Keywords:* radiative heat transfer, reacting flows, CFD, WSGG, RCSLW

---

## PROGRAM SUMMARY

*Program Title:* RadLib

*CPC Library link to program files:* (to be added by Technical Editor)

*Developer's repository link:* <https://github.com/BYUignite/radlib>

*Code Ocean capsule:* <https://codeocean.com/capsule/0997975/tree>

*Licensing provisions(please choose one):* MIT

*Programming language:* C++, Fortran, Python

*Nature of problem(approx. 50-250 words):*

Radiative heat transfer in combustion CFD problems is typically neglected or over-

---

\*Corresponding author.

*Email address:* [davidlignell@byu.edu](mailto:davidlignell@byu.edu) (David O. Lignell)

simplified, resulting in significant error and inaccuracy in combustion simulations. Radiation modeling, however, often requires a high degree of specialization due to its complexity and the challenges associated with implementation in existing CFD codes, which presents a substantial obstacle to researchers who wish to address the inaccuracies introduced by insufficient radiative heat transfer modeling in combustion simulations.

*Solution method (approx. 50-250 words):*

We present RadLib, an open-source C++ library of validated radiation property models that can be applied alongside various RTE solution methods to ease some of the obstacles associated with radiation modeling for combustion CFD. The package includes C++, Fortran, and Python interfaces, several illustrative examples with a provided ray-tracing solver and an integrated example using Fire Dynamics Simulator (FDS). RadLib can also be expanded to include additional radiation property models and interfaces.

*Additional comments including restrictions and unusual features (approx. 50-250 words):*

The library is intended to be used in Linux-like terminal applications.

## 1. Introduction

Modeling radiative heat transfer in participating media in high temperature systems is a challenging problem. Combustion is one of the key radiative transfer applications, and combustion CFD is uniquely challenging because it involves numerous tightly coupled physical phenomena—including multi-component mass transfer, convective and radiative heat transfer, turbulent fluid dynamics, multi-phase and particle flows, and complex chemical reaction kinetics—that span many orders of magnitude in both length and time scales. Accurate radiation modeling often complicates combustion simulations because it can be difficult to implement and computationally expensive relative to the overall simulation cost. Radiative heat transfer modeling in combustion systems is frequently neglected or oversimplified, resulting in significant errors flame temperatures [1]. Additionally, some late-stage flame phenomena, particularly soot behavior and flame sheet breakthrough, increasingly depend on and influence the magnitude of radiative heat losses and are difficult to simulate accurately without robust radiation modeling [2]. These problems motivated development of the RadLib library, which implements three radiation property models with C++, Python, and Fortran interfaces and provides a framework for additional models and further devel-

opment, giving researchers convenient access to advanced radiation property modeling tools.

The core mechanisms of radiative phenomena are physically and mathematically complex. Unlike other modes of heat transfer, radiation is governed by the radiative transfer equations (RTE), a set of integro-differential equations that depend on both direction and wavelength. Computational radiation solvers require two distinct but interconnected parts: (1) a solution approach for the radiative transfer equations (RTE) and (2) a radiative property model. The complexity, implementation, and computational cost of these two parts can vary widely depending on the models chosen. For example, the optically thin approximation for solution of the RTE is trivial, while the discrete ordinates model (DOM) and reverse Monte Carlo ray tracing (RMCRC) model, among others, are significantly more involved. Similarly, radiation property models range from simple correlations for computing mean absorption coefficients to gray gas models, including the weighted sum of gray gases (WSGG) model, to more advanced spectral line-weighted-sum-of-gray-gases (SLW) models to full line-by-line (LBL) treatment. In practical engineering simulations, the solution of the RTE is often the most complex and costly part of radiative simulation, but advanced property models such as the Rank Correlated SLW (RCSLW) model, discussed in Section 2.3, are nontrivial to understand, implement, and validate. RadLib addresses the second part of the radiation solver requirements by providing a set of implemented and validated radiation property models that can be applied alongside various solution approaches for the RTE.

For an absorbing, emitting, and non-scattering medium (considered here), the RTE solved for the intensity  $I$  at a specified wavenumber  $\eta$  in unit direction  $\mathbf{s}$  is described by

$$\frac{dI_\eta}{ds} = -\kappa_\eta I_\eta + \kappa_\eta I_{b,\eta}, \quad (1)$$

where  $I_\eta$  is the spectral radiative intensity,  $I_{b,\eta}$  is the blackbody spectral radiative intensity (or Planck function),  $\kappa_\eta$  is the spectral absorption coefficient of the medium, and  $s$  is a path length along direction  $\mathbf{s}$ . Solving the RTE requires information about the radiative properties of the materials and media in the system. Radiative property data typically take the form of radiation absorption coefficients  $\kappa$ , which are provided by a radiation property model. Gas absorption spectra consist of millions of spectral lines corresponding to the individual quantum mechanical energy levels of gas molecules and depend

on the local thermochemical state of the system (e.g., temperature, pressure, and composition). Radiation property models are typically developed as correlations from high-resolution spectral databases, reducing the huge amount of spectral data contained in those databases and simplifying the evaluation of absorption coefficients [4].

The direct solution of the spectral RTE using so-called line-by-line (LBL) calculations, in which the RTE is solved for each individual spectral line, is computationally prohibitive for most practical configurations and used primarily for model validation. Simple band models rely on estimated or averaged line-of-sight property values that cannot be directly incorporated into the RTE. Modern band models require high-resolution databases and reorder emission levels rather than averaging across sequential absorption bands, but these can lose accuracy when applied to nonhomogeneous media and may still require large numbers of RTE evaluations [1].

Global models are an important class of radiation property models that use spectrally-integrated radiation properties [5, 2, 1]. Assuming spectrally uniform (gray) properties over a wavenumber region  $j$ , we can integrate Eq. 1 over a set of fixed wavenumber ranges  $\eta_j$  to obtain

$$\frac{dI_j}{ds} = -\kappa_j I_j + a_j \kappa_j I_b, \quad j = 0, 1, \dots, n, \quad (2)$$

where  $I_b$  is the total blackbody intensity,  $I_j$  is the total radiative intensity in the region defined by gray gas  $j$ ,  $\kappa_j$  is the spectrally integrated absorption coefficient for gray gas  $j$ , and  $a_j$  is a weighting factor defined by

$$a_j = \frac{\int_{\eta_j} I_{b,\eta} d\eta}{I_b}, \quad (3)$$

$$\sum_j a_j = 1. \quad (4)$$

Given spatial profiles of  $\kappa_j$  and  $a_j$ , Eq. 2 can be evaluated for each of the  $n$  gray gases. Normally, an additional “clear gas”,  $j = 0$ , is included to represent transparent windows in the spectrum for which  $\kappa_0 = 0$ . This gray gas approach allows calculation of the total radiative intensity  $I$  by summing the individual gray gas intensities:

$$I = \int_{\eta=0}^{\infty} I_{\eta} d\eta = \sum_{j=1}^n I_j. \quad (5)$$

The heat flux  $\mathbf{q}$  (in units of kW/m<sup>2</sup>) and volumetric radiative heat source  $Q$  (kW/m<sup>3</sup>) can be calculated by integrating over directional solid angles ( $s\Omega$ ) on the sphere and finding the divergence of the resulting vector field, respectively:

$$\mathbf{q} = \int_{4\pi} I(\mathbf{s})\mathbf{s}d\Omega. \quad (6)$$

$$Q = -\nabla \cdot \mathbf{q}. \quad (7)$$

Global models are especially attractive in computational heat transfer applications because they can provide good accuracy while limiting computational costs.

RadLib calculates radiation absorption coefficients and weighting factors for use in global radiation models. It can interface with various RTE solution approaches suitable for CFD applications and serves as a convenient access point for radiative property modeling. The RadLib library includes three property models that are fully implemented and validated, but it can also be expanded to include other radiative properties and model types.

## 2. Model descriptions

At present, RadLib includes three radiation property models of varying complexity: a Planck Mean (PM) absorption coefficients model, a weighted sum of gray gases (WSGG) model, and the rank-correlated spectral line-weighted-sum-of-gray-gases (RCSLW) model. These models were chosen for their relevance to practical radiative heat transfer simulations. They represent increasing levels of complexity, computational cost, and accuracy. Each model is discussed in more detail in the following sections.

Radiation absorption coefficients are typically calculated via correlations developed from high-resolution spectral databases like RADCAL, HITRAN, and HITEMP [6, 3] that relate spectral line strength to properties such as temperature, pressure, and gas composition [4]. At present, RadLib considers up to four gas species (H<sub>2</sub>O, CO, CO<sub>2</sub>, and CH<sub>4</sub>), depending on the model, and soot. The property models implemented in RadLib apply only to non-scattering media. Table 1 summarizes RadLib’s three radiative property models and the thermodynamic conditions under which they apply.

### 2.1. Planck Mean absorption coefficients

The Planck Mean (PM) model is the simplest of the three models implemented. This model assumes a single gray gas (with no transparent gas) and

Model	T range	P range	Gas species	Refs.
PM	300–2500 K	1 atm	H <sub>2</sub> O, CO <sub>2</sub> , CO, CH <sub>4</sub>	[7]
WSGG	300–2400 K	0.01-60 atm·m	H <sub>2</sub> O, CO <sub>2</sub>	[15, 14]
RCSLW	300–3000 K	0.1–50 atm	H <sub>2</sub> O, CO <sub>2</sub> , CO	[17]

Table 1: Summary of radiative property models and ranges of applicability. For the WSGG model the pressure range is given in terms of the pressure-path length product.

computes the absorption coefficient as a function of temperature, pressure, and gas composition. The PM absorption coefficient is a Planck-function-weighted average absorption coefficient.

The version of the PM model implemented in RadLib comes from the Turbulent Nonpremixed Flames (TNF) workshop [7], a long-running collaboration between experimental and computational researchers in turbulent combustion [8, 9]. The workshop includes a number of laboratory jet flames that have been extensively characterized—including temperature, velocity, and composition profiles—and serve as target flames against which computational scientists can validate models and simulations. The PM model implemented in RadLib is the model advocated by the TNF workshop and, as a result, widely used in turbulent combustion research. For each chemical species considered, the PM model provides the absorption coefficient as a fourth or fifth order polynomial fit in one of two temperature ranges to  $\kappa(T)$  values computed from the RADCAL database [6]. The model accommodates temperatures between 300 K and 2500 K and considers the chemical species CO<sub>2</sub>, H<sub>2</sub>O, CO, CH<sub>4</sub>. CO, CH<sub>4</sub> contribute significantly less to radiative absorption and emission than CO<sub>2</sub> and H<sub>2</sub>O, but the TNF Workshop radiation model includes them because CH<sub>4</sub> and syngas (which consists of CO and H<sub>2</sub>) are common fuels in combustion applications and so are present in high concentrations in the fuel streams of several TNF target flames. Additionally, CO is also a common species in rich flame regions and is also included in the RCSLW model.

The PM model is not as accurate as the other two models considered, as illustrated by the example cases in Section 5. It is implemented in RadLib primarily for comparison and evaluation against other radiation property models because of its relatively common use in combustion simulations. The PM model reportedly overpredicts radiative losses and underpredicts flame temperature by as much as 100 K or more [10, 11, 12], though this depends

strongly on the geometric configuration of the simulation. Accurate results have been reported for hydrogen jet flames [13].

The PM model is most often used in conjunction with the optically thin approximation for solving the RTE, in which case the radiative source term of the energy transport equation reduces to an algebraic expression and the overall computational cost of the radiative treatment is negligible in comparison to other aspects of reacting flow simulations. Many smaller combustion configurations are radiatively thin and experience minimal radiative heat loss; non-sooting laboratory-scale research jet flames, for example, tend to exhibit radiative losses of around 5%. At low levels of radiative heat loss, the accuracy of the radiation model is not as crucial, and simpler radiative property models like the PM model may be appropriate.

## 2.2. Weighted sum of gray gases (WSGG)

Weighted sum of gray gases (WSGG) models generate radiation absorption coefficients for use with the spectrally integrated RTE (Eq. 2). RadLib implements the WSGG model presented by Bordbar et al. [14, 15]. This model computes emissivity for varying gas temperature, mixture composition, and path length using the HITEMP 2010 database [3]. The  $k_j$  and  $a_j$  are then correlated to these results using polynomial fits summarized below. The model considers mixtures of gaseous  $\text{CO}_2$  and  $\text{H}_2\text{O}$ , the two most significant radiatively participating species in most combustion environments, using four gray gases and one clear gas. Absorption coefficients are calculated by

$$\kappa_j = \sum_{k=0}^4 d_{j,k} M_r^k, \quad (8)$$

where  $\kappa_j$  is the absorption coefficient for gray gas  $j$ ,  $d_{j,k}$  is a correlated model coefficient, and  $M_r$  is the molar ratio  $x_{\text{H}_2\text{O}}/x_{\text{CO}_2}$ . The weight factors are calculated by

$$a_j = \sum_{k=0}^4 b_{j,k} T_r^k, \quad (9)$$

where  $a_j$  is the weighting factor for gas  $j$ ,  $b_{i,j}$  is computed as shown below, and  $T_r$  is a scaled temperature equal to  $T/T_{ref}$  with  $T_{ref}=1200$  K. The valid temperature range of the model is 300-2400 K; temperatures outside this range use the value at the respective bound. The  $\kappa_j$  values are not temperature dependent. The  $a_j$  values show a continuing trend as the temperature

increases past 2400 K up to 3000 K, suggesting possible use of the model at these temperatures. However, some of the  $a_j$  become slightly negative above  $\sim 2800$  K as the upper  $M_r$  bound is approached. The pressure range of the model is given in terms of the pressure-path length product with values from 0.01-60 atm·m. The value of  $b_{i,j}$  is calculated by

$$b_{j,k} = \sum_{i=0}^4 C_{j,k,i} M_r^i, \quad (10)$$

where  $C_{j,k,i}$  is a correlated model coefficient. The model coefficients  $d_{j,k}$  and  $C_{j,k,i}$  are provided by Bordbar et al. [14, 15], but updated values are used in RadLib.

This particular WSGG model was chosen for RadLib for its performance, accuracy, and flexibility. Most WSGG models are limited to specific values of the molar H<sub>2</sub>O–CO<sub>2</sub> ratio, or to a limited range of values. This is true of Bordbar et al.’s 2014 model [14], which used correlations valid for  $0.01 \leq M_r \leq 4$ . That paper summarizes a number of WSGG models and gives the applicable molar ratio range for several recent WSGG model versions. Bordbar et al. [15] extended the molar ratio range to arbitrary values by interpolating  $\kappa_j$  and  $a_j$  between the pure component values and the corresponding limit on  $M_r$  for values outside of the correlated range, and that is the model implemented here.

### 2.3. Rank Correlated SLW (RCSLW)

The spectral line-weighted-sum-of-gray-gases (SLW) model represents a family of global approaches to radiative heat transfer in high-temperature gases that also includes the absorption distribution function (ADF) and full spectrum  $k$ -distribution (FSK) models, all of which are based on the same fundamental principle in modeling the gas absorption spectrum [16]. In order to extend their spectral models from isothermal, homogeneous composition gases to non-isothermal, non-homogeneous composition gases, these models use a reference approach in which radiative properties at local gas states are computed with respect to properties at a reference state. Such approaches, however, generally lack consistent reference states and can yield significant errors in cases with large spatial temperature gradients [17]. The Rank Correlated SLW (RCSLW) model is a unique extension of the generalized SLW model that does not require a specified gas reference state.

The RCSLW model was chosen for RadLib for its accuracy and performance compared to other SLW and WSGG modeling approaches. A recent comparison of SLW modeling approaches revealed that “the Rank Correlated SLW model is the most robust of all models, and demonstrates that it can achieve accurate solutions with as few as 3–5 gray gases” [18]. The literature indicates that the RCSLW model has not yet been applied to turbulent combustion simulations [1, 19]. We provide an example below using the Fire Dynamics Simulator (FDS) [20]. Other SLW models have been applied to gas–soot mixtures [21, 22] and high-temperature non-isothermal gases [23, 24] with results that suggest their good applicability to combustion systems.

RadLib implements the RCSLW method presented by Solovjov et al. [17] as method I.2.2, which gives the best and most consistent results of the SLW methods discussed in the aforementioned study. A summary of the general SLW method and the RCSLW method are presented here, but more detailed information about these and other SLW methods can be found in the literature [25, 21, 26, 23, 27, 16, 17, 28].

SLW and WSGG models are similar in that they approximate real gas mixtures with a set of radiatively gray gases, but differ in the way that the gray gases are constructed. In traditional WSGG models, the component gases are only conceptually gray, and the absorption coefficients and weights are determined empirically [18]. In SLW approaches, however, the gases are gray in a given spectral band by construction. Rather than defining a gray gas  $j$  by integrating over a band of sequential wavenumbers  $\eta$  (which may have highly variable absorption coefficients), SLW models define a gray gas  $j$  by integrating over a set of nonsequential wavenumbers that correspond to a given band of the absorption cross section  $C_\eta$  with values constant to within the width of the band.

The absorption cross section is related to the absorption coefficient by  $\kappa_\eta = C_\eta N$ , where  $N$  is the molar density of the radiatively participating gas. Using Solovjov’s notation in [17],  $\Delta_j = \{\eta : \tilde{C}_{j-1} < C_\eta < \tilde{C}_j\}$  is defined as the set of wavenumbers that constitute the gray gas  $j$ , where  $\tilde{C}$  denotes a cross section boundary between two gray gases. Hence, in SLW models, the gases in a given band are gray to within the width  $\tilde{C}_j - \tilde{C}_{j-1}$ .

The gray gas weight  $a_j$  is the fraction of blackbody emission from the set of wavenumbers  $\Delta_j$  that correspond to a given cross-section band  $j$ . Weights are computed using the absorption line blackbody distribution function (ALBDF) [29], which gives the fraction of total blackbody emission from  $\eta$  corresponding to absorption cross sections smaller than an arbitrary ab-

sorption cross-section  $C$ :

$$F(C, \phi, T) = \frac{1}{\sigma T^4} \int_{\{\eta: C_\eta(\eta, \phi) < C\}} E_b(\eta, T) d\eta, \quad (11)$$

where  $\phi$  represents the thermodynamic state,  $\sigma$  is the Stefan-Boltzmann constant,  $T$  is temperature, and  $E_b(\eta, T)$  is the blackbody emission at a given wavenumber  $\eta$  and temperature  $T$ . As a result, a specific gray gas weight  $a_j$  can be calculated as the difference between the ALBDF values at its cross-section boundaries:

$$a_j = F(\tilde{C}_j, \phi, T) - F(\tilde{C}_{j-1}, \phi, T). \quad (12)$$

Note that  $F$  varies between zero and one and is monotonic in  $C$ , which permits calculation of an inverse ALBDF  $C(F, \phi, T)$ .

For multicomponent gas mixtures, the mixture absorption cross section  $C_\eta$  is defined as a weighted sum of its component absorption cross sections [25]. In RadLib, the RCSLW implementation considers  $\text{H}_2\text{O}$ ,  $\text{CO}_2$ , and  $\text{CO}$ , for which the mixture absorption cross section for a given gray gas is given by

$$C_\eta = x_{\text{CO}_2} C_{\text{CO}_2, \eta} + x_{\text{H}_2\text{O}} C_{\text{H}_2\text{O}, \eta} + x_{\text{CO}} C_{\text{CO}, \eta}, \quad (13)$$

where  $x$  denotes mole fraction. Assuming that the absorption cross sections of each species are statistically independent, the mixture ALBDF for a given gray gas can be computed using the multiplication method [25]:

$$F_\eta(C_\eta) = F_{\text{CO}_2, \eta} \left( \frac{C_\eta}{x_{\text{CO}_2}} \right) F_{\text{H}_2\text{O}, \eta} \left( \frac{C_\eta}{x_{\text{H}_2\text{O}}} \right) F_{\text{CO}, \eta} \left( \frac{C_\eta}{x_{\text{CO}}} \right). \quad (14)$$

Note that the  $\phi$  and  $T$  arguments of  $F$  are omitted from Eq. 14 for clarity.

The spectrally integrated RTE (Eq. 2) assumes the sets  $\Delta_j$  are independent of spatial position  $\mathbf{x}$ , but  $C_\eta$  depends on the thermodynamic state (denoted by vector  $\phi$ ), which does vary spatially. Hence, a spatially-fixed  $\Delta_j$  with spatially varying  $\phi$  implies a spatial variation in  $C_j$  and  $\tilde{C}_j$ . The RCSLW model uses the notion of rank correlation to handle this spatial variation in the ALBDF. Consider two positions with thermodynamic states  $\phi_1$  and  $\phi_2$  with corresponding absorption cross section spectra  $C_\eta(\eta, \phi_1)$ , and  $C_\eta(\eta, \phi_2)$  and let  $\hat{C}_1 \equiv C_\eta(\hat{\eta}, \phi_1)$  and  $\hat{C}_2 \equiv C_\eta(\hat{\eta}, \phi_2)$  denote the cross sections at some wavenumber  $\hat{\eta}$ . For each spectrum, we define the set of wavenumbers that

give cross sections less than  $\hat{C}$  as

$$H_1 = \{\eta : C_\eta(\eta, \phi_1) < \hat{C}_1\}, \quad (15)$$

$$H_2 = \{\eta : C_\eta(\eta, \phi_2) < \hat{C}_2\}. \quad (16)$$

If  $H_1 = H_2$  for an arbitrary  $\hat{\eta}$ , then the spectra  $C_\eta(\eta, \phi_1)$  and  $C_\eta(\eta, \phi_2)$  are said to be rank correlated.

The RCSLW model uses rank correlation as follows. Consider Eq. 11 evaluated at an arbitrary reference temperature  $T_r$  for thermodynamic states  $\phi_1$  and  $\phi_2$  as detailed above:

$$F(\hat{C}_1, \phi_1, T_r) = \frac{1}{\sigma T_r^4} \int_{H_1} E_b(\eta, T_r) d\eta, \quad (17)$$

$$F(\hat{C}_2, \phi_2, T_r) = \frac{1}{\sigma T_r^4} \int_{H_2} E_b(\eta, T_r) d\eta. \quad (18)$$

Since  $C_\eta(\eta, \phi_1)$  and  $C_\eta(\eta, \phi_2)$  are rank correlated (by definition),  $H_1 = H_2$  and we have

$$F(\hat{C}_1, \phi_1, T_r) = F(\hat{C}_2, \phi_2, T_r). \quad (19)$$

Recall that the ALBDF can be inverted, so if  $\hat{C}_1$  and  $\phi_1$  are known, we can compute  $F = F(\hat{C}_1, \phi_1, T_r)$  and then invert  $F$  to obtain  $\hat{C}_2$  at  $\phi_2$ . Note that Eq. 19 holds for arbitrary states  $\phi_1$  and  $\phi_2$ , so any known  $F = F(C, \phi, T)$  can be inverted to get  $C$  at the corresponding state  $\phi$ .

Given the concepts summarized above, the RCSLW model is applied to a problem of interest to calculate radiation absorption coefficients and weights as follows:

1. Specify a reference temperature  $T_r$  as the average temperature on the domain of interest [21]. Note that this is not the same as specifying a reference state  $\phi = \phi_r(T_r, x_r, P_r)$  as in done for SLW reference approaches.
2. Specify a collection of  $F_j$  points and  $\tilde{F}_j$  boundary values such that  $F_j$  lies between  $\tilde{F}_j$  and  $\tilde{F}_{j-1}$ . These apply to all spatial positions.
3. Invert the ALBDF to calculate  $C_j$  and  $\tilde{C}_j$  at the corresponding thermodynamic state  $\phi$  and any spatial position where  $C_j = C(F_j, \phi, T_r)$  and  $\tilde{C}_j = C(\tilde{F}_j, \phi, T_r)$
4. Compute the gray gas absorption coefficients  $\kappa_j = C_j N$ .

5. Compute the gray gas weights  $a_j = F(\tilde{C}_j, \phi, T) - F(\tilde{C}_{j-1}, \phi, T)$  (Eq. 12) with the  $C_j$  and  $\tilde{C}_j$  values calculated in Step 3, the local thermodynamic state  $\phi$ , and the local temperature  $T$ .

The ALBDF data for H<sub>2</sub>O, CO<sub>2</sub>, and CO—valid for pressures between 0.1 atm and 50 atm and temperatures between 300 K and 3000 K—are provided by Pearson et al. [29] and can be accessed in both correlated and tabulated form at [30]. Temperatures outside the stated range use the value at the respective bound. RadLib uses the tabulated data coupled with multilinear interpolation; both the tabulated data and the multilinear interpolator are included with the RadLib package as part of the RCSLW method.

#### 2.4. Soot

Soot is accounted for in all three implemented models. Soot particles are assumed to be unagglomerated spheres that absorb and emit radiation at all wavelengths such that their optical properties can be determined using the Rayleigh small particle limit. This assumption implies that radiation scattering may be neglected because unagglomerated soot particles in the Rayleigh regime are still small relative to the wavelength of infrared radiation in flames [31, 21]. The spectral soot absorption coefficient is given by

$$\kappa_{s,\eta} = C_0 f_v \eta, \quad C_0 = \frac{36\pi n k}{(n^2 - k^2 + 2)^2 + 4n^2 k^2}, \quad (20)$$

where  $n$  and  $k$  are the real and imaginary parts of the soot complex index of refraction, respectively, and  $f_v$  is the soot volume fraction [21, 2]. Various values for the refraction index have been proposed and applied [32, 33, 34, 35, 36, 37, 38]. RadLib uses the values  $n = 1.75$  and  $k = 1.03$  [38], resulting in a value of  $C_0 = 7.03$ , which is nearly the same as the value of  $C_0 = 7.0$  used by Solovjov and Webb [21] to study radiative transfer in sooty gas mixtures. The Planck mean and Rosseland mean soot absorption coefficients are given in [2] as  $\kappa_s = 3.83 f_v C_0 T / C_2$  and  $\kappa_s = 3.60 f_v C_0 T / C_2$ , respectively. Due to the small difference between the coefficients in these two expressions, the mean value suggested by [2, 39] is used in RadLib’s soot calculations:

$$\kappa_{soot} = 3.72 \frac{f_v C_0 T}{C_2}, \quad (21)$$

where  $T$  is the temperature and  $C_2 = 0.014388$  m K is a Planck function constant [2].

In the Planck Mean model, which treats a gas mixture as one gray gas, the soot absorption coefficient calculated from Eq. 21 is simply added to the gas absorption coefficient. Using the given values of  $C_0$  and  $C_2$  above, the expression for the soot absorption coefficient simplifies to  $\kappa_s = 1817f_vT$  with units of  $\text{m}^{-1}$ .

In the WSGG model, the soot absorption coefficient is also computed using Eq. 21 but then added to each of the gray gases separately [40]. Because soot radiates across all wavelengths, its absorption coefficient is added to the value of the clear gas in addition to the values of the four gray gases. The gas weights  $a_j$  are not changed. This model yields the expected behavior in the soot-only and gas-only limits.

The WSGG soot treatment can be applied to the RCSLW model as well. Alternatively, the RCSLW model's formulation permits a spectral soot treatment in the same manner as the gas species [21]. Calculation of the soot ALBDF is facilitated by the simple  $\eta$  dependence of  $\kappa_{s,\eta}$  in Eq. 20. The fraction of total blackbody emission at wavenumbers below  $\eta$  is computed directly using a series expansion presented by Chang and Rhee [41]. The soot ALBDF is then included in the product of species ALBDFs to obtain the mixture ALBDF, as in Eq. 14.

### 3. Software Description

RadLib is an object-oriented C++ library that includes C++, Python, and Fortran interfaces. Upon initial download, the RadLib package contains four subdirectories:

- `src` contains the RadLib source code;
- `examples` contains instructive example cases, including a simple interface and solver for a parallel planes geometry;
- `data` contains ALBDF data tables required for the RCSLW model; and
- `docs` contains files used to optionally generate code documentation with Doxygen.

An additional directory, `installed`, is created and populated with RadLib's executables and header files during installation if no other installation location is specified. The `src` and `examples` directories are further divided into `c++`, `python`, and `fortran` subdirectories to differentiate between interfaces.

RadLib installation is automated with CMake. Inside the downloaded `radlib` folder, the user must create a `build` directory and navigate into it. From there, the user executes the following commands in order:

1. `cmake ..`
2. `make`
3. `make install`

Project options can be specified by editing the top-level `CMakeLists.txt` file where the options are clearly marked. These can also be specified at the command line. Options include specifying the system installation location, which defaults to `radlib/installed`; options to build the Python and Fortran interfaces; options to build examples for C++, Python, and Fortran; and an option to build the documentation. Refer to the included `README` files for additional information.

Following successful installation, the installation folder will contain four directories: `cmake` contains relocatable CMake files for downstream developer use; `include` contains the C++ header files and a Fortran module file; `lib` contains library files for each interface, including the python module files; and `rcslw_data` contains the binary data files used by the RCSLW model, each of which contains the tabulated ALBDF functions for a given species at a given pressure (in units of atm) as indicated by the file name. If the Python interface is built, the location of the installed Python package must be added to the `PYTHONPATH` environment variable. A command instructing the user how to do this is provided at the end of the installation. The following outline further illustrates the organization of the installation folder and file locations therein:

- `cmake`
  - `radlib`
    - \* `radlib.cmake`
  - `radlib_fortran`
    - \* `radlib_fortran.cmake`
- `include`
  - `rad_planck_mean.h`
  - `rad_wsgg.h`

- rad\_rcslw.h
- rad\_module.mod
- lib
  - libradlib.a
  - libradlib\_fortran.a
  - python[version]
    - \* site-packages
      - pyrad.cpython-[system architecture].so
- rcslw\_data

To use RadLib in C++ code, the user must include the header file for the desired radiation model, e.g., `#include "rad_rcslw.h"`, in their code. Compilation requires specification of the header and library directory locations and linking against the installed library (`libradlib.a`). In Fortran, a `use rad_module` statement provides access to the required interface functions. To compile, the module and library locations must be specified and the code linked against both `libradlib.a` and `libradlib_fortran.a`. The Python interface functions are loaded from the `pyrad` module, as in `from pyrad import pyrad_rcslw`. The examples included with the RadLib package and discussed in Section 4 demonstrate these usages.

Figure 1 illustrates the basic structure of using RadLib in a generic one-dimensional RTE solution. The RadLib library generates absorption coefficients and their weighting factors for use within an appropriate RTE solver. A user first creates a radiation object, and then makes calls to one of two primary functions: `get_k_a()` or `get_k_a_oneband()`. These two functions take the arguments for temperature (K), pressure (Pa), soot volume fraction, and mole fractions of H<sub>2</sub>O, CO<sub>2</sub>, CO, and CH<sub>4</sub>. The CO and CH<sub>4</sub> mole fraction parameters have default values of zero and do not need to be specified for models that do not make use of them (see Table 1). The `get_k_a()` function computes a vector of absorption coefficients and a vector of weight factors in which each element corresponds to one of the gray gases considered in the model (with the clear gas in the first position). The PM model only considers one gray gas and thus returns vectors containing one element each. The `get_k_a_oneband()` function computes the absorption coefficient and weight factor as scalar values for a single gray gas whose index (starting

at zero for all interfaces) is provided as an additional argument. This option to compute the properties for a single gas/band can be important for efficient implementation in some solvers, e.g., in the Fire Dynamics Simulation (FDS), discussed below [20]. The absorption coefficients and weights are set through the function argument list for the C++ and Fortran interfaces and as return values for the Python interface. Additional details are included in the program documentation and code listing.

The RadLib source code is build around a base class called `rad` from which the individual property models, e.g., `rad_rcslw`, inherit. To extend RadLib to include new radiative property models, a user would create a new derived class for the model that inherits from the `rad` base class. The interface functions `get_k_a` and `get_k_a_oneband` would be reimplemented in the new model. Additional functions and capabilities could be added as desired. The Fortran and Python interface codes consist of wrapper functions to the underlying C++. These can be easily extended by paralleling the existing interface functions.

#### 4. Examples

The RadLib package includes several example cases that illustrate the behavior of the models and interfaces. The examples compare the PM, WSGG, and RCSLW models via output heat flux  $q$  or volumetric heat source  $Q$  in one-dimensional configurations with varying gas compositions and temperatures. The RTE is solved between two parallel plates with a ray-tracing code, included in the RadLib package. Results for each case are presented alongside the line-by-line (LBL) data from the respective references.

Table 2 summarizes the example cases. Each case is labeled according to its source—Solovjov et al. [17] (S), Bordbar et al. [15] (B), or Solovjov et al. [21] (Sb)—and the number of each example corresponds to the example number in its respective reference. Each example case consists of one or more gas layers (“slabs”) bounded by black walls. Example S1 consists of two adjacent gas layers with identical species compositions: one hot layer of constant thickness and one cold layer of varying thickness. In Example S2, the two gas layers are isothermal but differ in the value of the CO<sub>2</sub> mole fraction, where the layer thickness of the “thin” slab (with the smaller CO<sub>2</sub> mole fraction) varies. Example S3 applies parabolic temperature and H<sub>2</sub>O mole fraction profiles across a single gas layer. Example S4 divides the gas into three equally-spaced layers and applies a triangular temperature

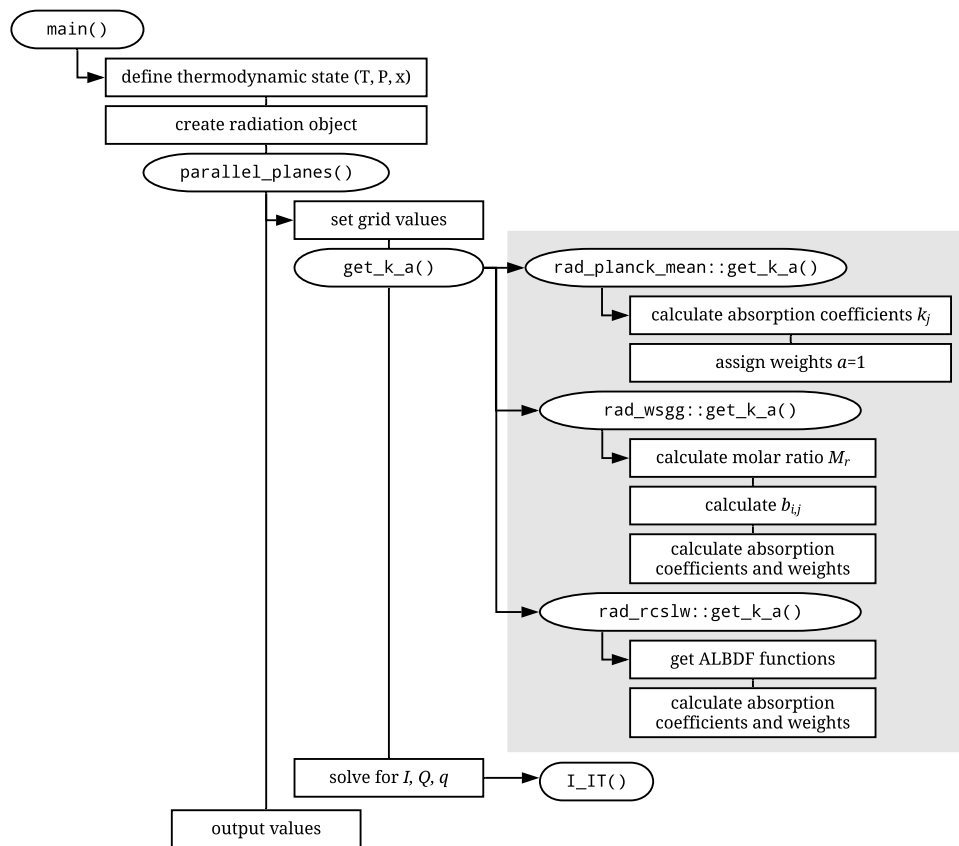


Figure 1: Example workflow diagram. Highlighted areas are part of the RadLib library; other areas represent example infrastructure for using the package.

Example	T(K)	$x_{H_2O}$ $x_{CO_2}$ (mole frac.)	L (m)	$T_{walls}$ (K)	Ref.
S1	$T(x < 0.5) = 2000; T(x > 0.5) = 300$	$x_{CO_2} = 0.1, x_{H_2O} = 0.2$	0.5-2.5	cold, cold	[17]
S2	T=1000	$x_{CO_2}(x < 0.5) = 0.4, x_{CO_2}(x > 0.5) = 0.1$ $x_{H_2O} = 0.0$	0.5-2.5	cold, cold	[17]
S3	$T(x) = 4000x(L-x)/L^2 + 800$	$x_{H_2O}(x) = 0.8x(L-x)/L^2 + 0.12$ $x_{CO_2} = 0$	1	800, 800	[17]
S4	middle third triangular to 2500	$x_{H_2O} = 0.1, x_{CO_2} = 0$	0.3	500, 500	[17]
S5	$T(x) = 1000 + 500 \cos(\pi x/L)$	$x_{H_2O} = 0.1, x_{CO_2} = 0$	2	1500, 500	[17]
B3	$T(x) = 400 + 1400 \sin(\pi x/L)^2$	$x_{H_2O}(x) = 0.0001 + 0.9999 \sin(\pi x/L)^2$ $x_{CO_2} = 1 - x_{H_2O}$	1	400, 400	[15]
Sb1	T = 1000	$x_{H_2O} = 0.2, x_{CO_2} = 0.1, x_{CO} = 0.03$	1	cold, cold	[21]

Table 2: Summary of example cases. All cases use  $P = 1$  atm and black walls.

profile to the middle layer and a constant temperature to the two outer layers. Example S5 uses a half-sinusoid temperature profile that decreases from 1500 to 500 K applied to a single gas layer of constant composition. Example B3 has symmetric temperature and H<sub>2</sub>O mole fraction profiles with central peaks of 1800 K and 1, respectively (with  $x_{CO_2} = 1 - x_{H_2O}$ ). Example Sb1 consists of a single gas with a uniform temperature and composition profile and soot radiation.

The examples are provided with the RadLib code and implemented in both C++ and Python. A Jupyter notebook is provided with the Python examples that runs the examples, displays the plots, and saves the plots to PDF files. Python and Cython versions of the one-dimensional solver `parallel_planes.py` are provided for convenience.

These cases are intended to illustrate the use of the RadLib library and are not exhaustive. Details about these examples and their motivations can be found in their respective references. Comparison of these results to the LBL data, shown here, serve as model validation. For the WSGG and RCSLW models, direct comparison (not shown) of RadLib was made to examples presented in the model references with identical results (up to the resolution of the available data), which serves as verification of the implementation.

## 5. Results and Discussion

Figures 2 and 3 display comparative results for the PM, WSGG, and RCSLW models implemented by RadLib in the example case configurations summarized in Table 2. These plots are included to demonstrate the examples that are provided with the code, and to compare the models to give an indication of their relative accuracy. In all examples, the RCSLW model data

is computed using four gray gases ( $n = 4$ ) and one clear gas for consistent comparison to the WSGG model, with the exception of Examples S2 and S5, in which the number of gray gases in the RCSLW model is varied. The RCSLW model is initialized using the mean temperature and composition on the domain for all cases except Example S5, which uses the maximum temperature.

In general, the PM model performs poorly compared to the WSGG and RCSLW models and the LBL data. The results show that the PM model tends to exaggerate the trends displayed by the other models. The PM data mimics the shape of the other curves in Example S5 as well, but the curve is off-scale and omitted for clarity. For the PM model in Example S5,  $Q$  varies from around  $-80 \text{ kW/m}^3$  at  $x = 0$  to a peak of  $200 \text{ kW/m}^3$  at  $x=1.5 \text{ m}$  and drops to  $100 \text{ kW/m}^3$  at  $x = 2 \text{ m}$ . In Example S2, the PM value of  $q(L)/\sigma T^4$  is off the scale at an essentially constant value of unity. The PM absorption coefficient is  $27.4 \text{ atm}^{-1}\text{m}^{-1}$ , which results in optical thicknesses greater than 5.5 for the domain sizes considered in Example S2.

Example S3 illustrates that the PM model tends to overpredict radiative heat loss at high temperatures, which has been previously observed [10, 11, 12].

The WSGG model closely follows the trends of the LBL data for all examples, and in most examples gives reasonable quantitative agreement. This is especially true for Examples S2, S4, and B3. For example S5, the WSGG model shows peak errors of around 50%, and somewhat higher in Example S1. The heat flux near the boundaries in Example B3 is low by around 30%. The RCSLW model gives results in very close agreement to the LBL data for all examples. A notable exception is Example S2, where the heat flux at the right boundary is not well-predicted with four gray gases. The heat flux does converge to the LBL results when the number of gray gases increases. This behavior was not discussed in [17] where 24 gray gases were used. The WSGG model is very close to the LBL data for this case. The good agreement is likely a result of the simplicity of this case, which is isothermal with pure  $\text{CO}_2$  at uniform concentration in either of the two adjacent gas slabs. The RCSLW model is sensitive to the number of gray gases used, as illustrated in Figure 2 by Examples S2 and S5. The difference in accuracy between  $n = 2$  and  $n = 8$  gray gases is small for all of the example cases (not shown) and typically falls within the margin of error represented by the WSGG model's deviation from the LBL data. The RCSLW model also depends on the value of the chosen reference temperature that is used to

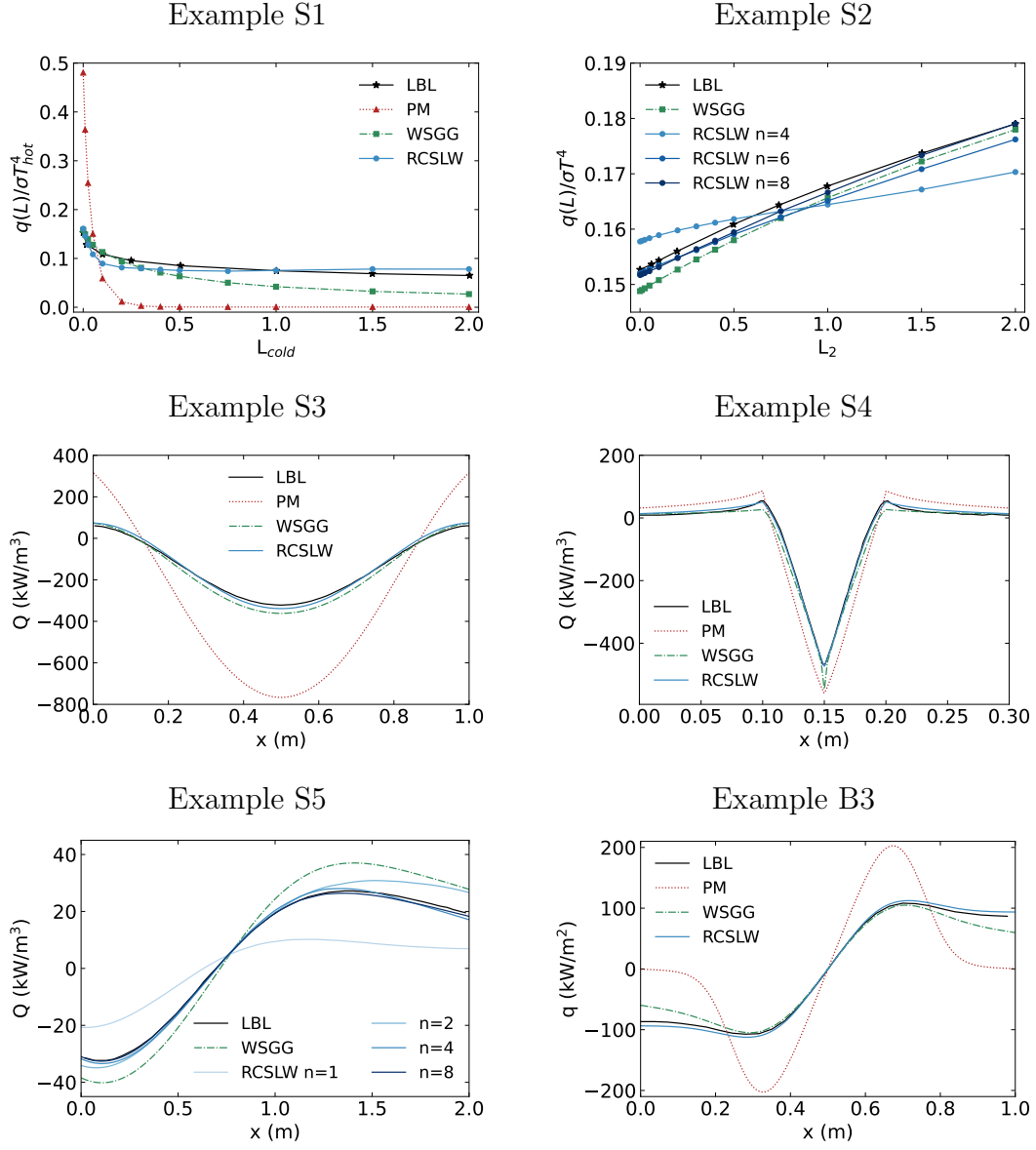


Figure 2: Results for Examples S1-S5 and B3 summarized in Table 2. In Examples S2 and S5,  $n$  refers to the number of gray gases considered in the RCSLW model.

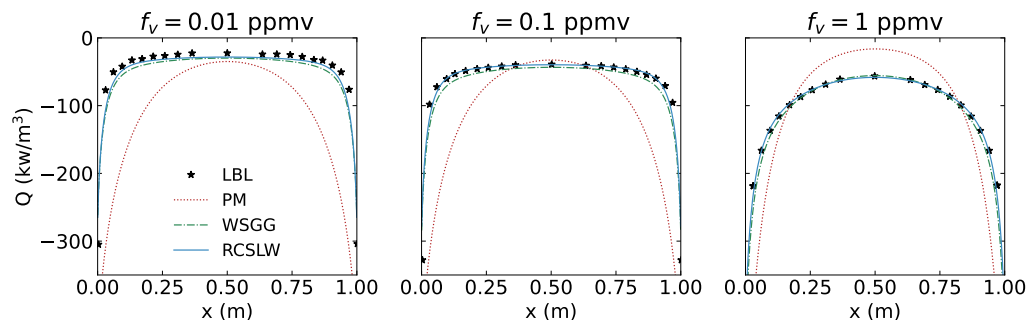


Figure 3: Results for Example Sb1 summarized in Table 2.

set the ALBDF grid. In Example S5, the RCSLW model does not converge to the LBL data at  $x > 0.5$  m when the domain average temperature is used.

Figure 3 shows the results from Example Sb1, which considers three magnitudes of the soot volume fraction in addition to the radiating gas. Both the WSGG and RCSLW models perform accurately in all three cases, but the PM model displays significant deviations from the LBL data. In sooting flames, soot acts as a significant source and sink of radiation, and its radiative properties differ significantly from those of the participating gaseous species. Soot reactions and transport are both sensitive to, and strongly influence local variations in, flame temperature and gas composition, forming a feedback loop in which accurate prediction of both gas and soot radiative properties becomes critical to predicting flame properties and behavior, particularly late-stage flame phenomena such as flame sheet breakthrough, smoke production, and extinction and reignition processes. As such, simpler models such as the PM model may fail to capture important subtleties in soot’s radiative behavior.

### 5.1. CFD Results

The RadLib model was coupled to the Fire Dynamics Simulator (FDS) code developed at NIST [20]. FDS is written in Fortran, and the Fortran interface of Radlib was used for simulations. FDS includes several radiative models, but the spectral WSGG model coupled to a finite volume discrete ordinates model is used here. This was done by editing the `radi.f90` file in FDS. A `use rad_module` statement is included there and the FDS functions `A_WSGG` and `KAPPA_WSGG` are replaced with calls to RadLib’s `get_k_a_oneband`.

The `oneband` version was used because FDS does an outer iteration over the bands/gases, computing properties at a given band for each grid point.

FDS includes a number of validation cases. Here, we compare to the FM Burner case. The configuration is a vertically fired gas burner with various fuels and with a coflow oxidizer stream of varying nitrogen dilution. The burner has outer and inner diameters of 15.2 and 13.7 cm, respectively, and is near the floor in the center of a 1.22 by 1.22 by 1.83 m tall compartment. The heat release rate was 10 kW and included a 1 kW pilot in a surrounding ring. The coflow oxidizer was fed through the floor. Simulations performed here used the ethylene fuel with 20.9% N<sub>2</sub> oxidizer (i.e., air). Further FDS model and case simulation details are provided in the FDS validation and user guides [20].

Figure 4 shows results of the simulation with comparison to experimental data. Three radiation models were included: the FDS default model, and the RCLW and WSGG models from RadLib (both using four gray gases and one clear gas). The FDS default model uses a single gray gas with a composition and temperature dependent absorption coefficient computed from RADCAL. The calculation depends on a user-specified radiation path length variable with a default value of 0.1 m, which is used in the FM Burner validation case. Further details are provided in the FDS user guide [20]. Figure 4a shows radial profiles of mean temperature at two vertical positions. The models produce maximum radial temperature differences at 1.5R of about 70 K (6%) between the RCLW and the WSGG at  $z=2.5D$ , and 50 K (6%) at  $z=3.5D$ . Figure 4b plots height versus radiative emission per unit length along the centerline with the spread in radiative emission around the peak values being 0.94 kW/m (8%).

## 5.2. Computational Cost

In addition to comparing model attributes and performance, we evaluated and compared the computational cost of the implemented radiation property models. Calculations were performed on a 4 GHz Quad Core Intel Core i7 iMac, version 10.15.7. The results, normalized by the cost of the WSGG model, are summarized in Figure 5. In the results presented, only the cost of evaluating the solution was included; model initialization and input/output costs were neglected. In the results including the ray-tracing solver, the same number of rays and grid points is used in all calculations.

Figure 5a displays the relative cost to compute the gas properties  $\kappa$  and  $a$ , represented by the time required to execute the C++ function `get_k_a()`,

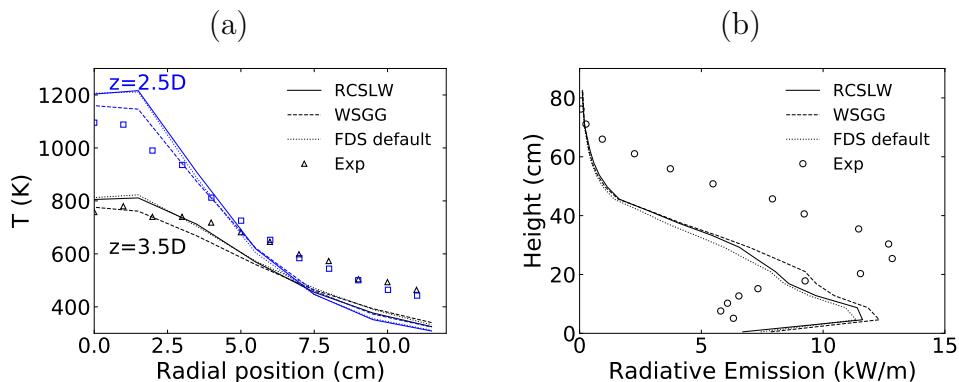


Figure 4: Radial profiles of mean temperature at two heights (a) and height versus radiative emission (b) for FDS simulations of the FM Burner validation case comparing three models to experimental data.

averaged over one million evaluations. The results for each model are normalized by the WSGG model, which required an average of  $8.0E-7$  s. Relative to the WSGG model, the cost to evaluate the gas properties with the PM model was 0.098. The RCSLW model was evaluated with  $n = 1, 2, 4,$  and  $8$  gray gases, which resulted in relative costs of 1.9, 4.9, 9.4, and 18, respectively, which is very nearly proportional to the number of gray gases considered.

Figure 5b shows the cost to evaluate Example S3, which involves both evaluation of the gas properties and solution of the RTE using the provided ray-tracing solver. This is relevant because radiative property calculations are rarely done in isolation, but are part of a larger RTE solution, so that overall cost differences may be smaller than those of the property evaluations alone. This is consistent with the results of Figure 5b and as follows. Relative to the WSGG model, which required 0.0079 s, the model costs for the PM model and the RCSLW model with  $n = 1, 2, 4, 8$  gray gases was approximately 0.75, 1.1, 1.4, 1.9, and 2.9, respectively.

Cost comparisons were also attempted with Python, but meaningful results are difficult to obtain when mixing Python and C++. In particular, the cost of a single evaluation of the gas properties is small and evaluating the gas properties in a Python loop results in the loop itself appearing to dominate the computational cost. Comparison between Python and C++ for Example S3 is somewhat more meaningful, but even here, for the six cases considered in Figure 5 the cost only varied by about 4%, indicating that the

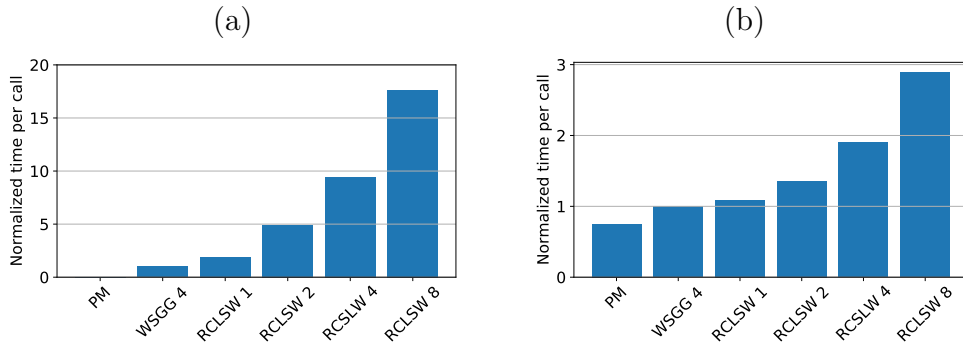


Figure 5: Relative computational cost to (a) evaluate gas properties only and (b) run Example S3, including the ray-tracing solver. Results are normalized by the cost of the WSSG model for each case.

computational cost is dominated by Python wrapper rather than by the underlying C++ model evaluations or solver. The cost of the WSGG model was 0.6 s, which is 7.6 times slower than the C++ version. It is possible that optimizing the Cython interface could improve the speed and relative cost of using Python with RadLib, but RadLib’s Python interface and examples are primarily intended to demonstrate the library’s use and provide a convenient interface rather than serve as a point of use for detailed CFD calculations.

The computational cost of the FDS simulations, relative to the default model are 1, 1.68, and 1.71 for the default, WSGG, and RCLSW model, respectively. This indicates that the cost is dominated by the radiative solver and not the computation of the radiative properties.

## 6. Conclusions

Radiative heat transfer phenomena are historically difficult to model and implement in CFD calculations due to their high level of conceptual and mathematical complexity and potentially large computational cost. Many combustion CFD studies either neglect radiative heat transfer or employ oversimplified models that do not accurately represent combustion systems. Most combustion processes of interest to engineers and researchers, however, involve significant radiative heat transfer, and simulations require robust radiative modeling, which includes both radiation property modeling and solution approaches for the radiative transfer equation, to yield accurate

results.

RadLib is a C++ library of radiation property models developed to facilitate implementing radiative property models in CFD simulations. At present, it includes three major radiation property models—Planck Mean (PM) absorption coefficients, the weighted sum of gray gases (WSGG) model, and the rank-correlation spectral line weighted-sum-of-gray-gases (RCSLW) model. Each of the implemented models has been validated and the library’s structure and functionality has been outlined. The library can be expanded to include additional property models.

In addition to the library itself, RadLib includes several illustrative example cases in a one-dimensional parallel planes geometry using a simple ray tracing solver to demonstrate use of the library and validate model implementation. Results are compared to line-by-line (LBL) solutions. In general, the RCSLW model outperforms both the PM and WSGG models in terms of accuracy at the expense of computational cost.

RadLib is intended as a convenient access point for researchers who require radiation property modeling tools for relatively high temperature CFD applications such as combustion but could potentially be applied to research problems involving radiative heat transfer in other fields as well. RadLib is designed to facilitate and simplify the process of implementing and using radiative property models; it consolidates various model types into a single library with a consistent framework, reducing some of the overhead associated with choosing, implementing, and testing radiation property models. Its framework can be used to implement and validate new models as well as compare existing models under consistent conditions. By facilitating model comparison through a common interface, RadLib can provide a practical means of testing specific modeling approaches without the restrictions imposed by large-scale CFD simulations.

## **7. Declaration of Competing Interests**

The authors declare that they have no known competing financial interests or personal relationships that could have appeared to influence the work reported in this paper.

## **Acknowledgements**

The authors extend special thanks to Hadi Bordbar for assistance with the WSGG model and to Vladimir Solovjov and Brent Webb for their insights

and assistance with the RCLW model. This research did not receive any specific grant from funding agencies in the public, commercial, or not-for-profit sectors.

## References

- [1] M. F. Modest, D. C. Haworth, Radiative Heat Transfer In Turbulent Combustion Systems: Theory and Applications, SpringerBriefs in Applied Sciences and Technology, Springer, 2016.
- [2] M. F. Modest, Radiative Heat Transfer, Third Edition, Academic Press, New York, 2013.
- [3] L. S. Rothman, I. E. Gordon, R. J. Barber, H. Dothe, R. R. Gamache, A. Goldman, V. I. Perevalov, S. A. Tashkun, J. Tennyson, HITEMP, the high-temperature molecular spectroscopic database, Journal of Quantitative Spectroscopy & Radiative Transfer 111 (15) (2010) 2139–2150. doi:10.1016/j.jqsrt.2010.05.001.  
URL <http://www.sciencedirect.com/science/article/pii/S002240731000169X>
- [4] H. Zhang, M. F. Modest, Evaluation of the Planck-mean absorption coefficients from HITRAN and HITEMP databases, Journal of Quantitative Spectroscopy & Radiative Transfer 73 (6) (2002) 649–653. doi:10.1016/S0022-4073(01)00178-9.
- [5] H. C. Hottel, A. F. Sarofim, Radiative Transfer, McGraw-Hill, 1967.
- [6] W. L. Grosshandler, RADCAL: A Narrow-Band Model for Radiation Calculations in a Combustion Environment: NIST technical note 1402.
- [7] TNF Workshop Radiation Models, <https://tnfworkshop.org/radiation/> (2021).
- [8] N. Smith, J. Gore, J. Kim, Q. Tang, TNF Workshop Radiation Models (2003).  
URL <https://tnfworkshop.org/radiation/>
- [9] R. S. Barlow, A. N. Karpetis, J. H. Frank, J.-Y. Chen, Scalar profiles and NO formation in laminar opposed-flow partially premixed methane/air

- flames, *Combustion and Flame* 127 (3) (2001) 2102–2118. doi:10.1016/S0010-2180(01)00313-3.
- [10] J. H. Frank, R. S. Barlow, C. Lundquist, Radiation and nitric oxide formation in turbulent non-premixed jet flames, *Proceedings of the Combustion Institute* 28 (1) (2000) 447–454. doi:10.1016/S0082-0784(00)80242-8.
- [11] X. Zhu, J. Gore, A. N. Karpetis, R. S. Barlow, The effects of self-absorption of radiation on an opposed flow partially premixed flame, *Combustion and Flame* 129 (3) (2002) 342–345. doi:10.1016/S0010-2180(02)00341-3.  
URL <http://www.sciencedirect.com/science/article/pii/S0010218002003413>
- [12] P. J. Coelho, O. J. Teerling, D. Roekaerts, Spectral Radiative Effects and Turbulence-Radiation-Interaction in Sandia Flame D, in: Barlow, Robert S., Pope, Stephan B., Masri, Assaad R., Oefelein, Joseph C. (Ed.), *The Proceedings of the Sixth International Workshop on Measurement and Computation of Turbulent Nonpremixed Flames*, 2002.
- [13] R. Barlow, N. Smith, J. Chen, R. Bilger, Nitric oxide formation in dilute hydrogen jet flames: isolation of the effects of radiation and turbulence-chemistry submodels, *Combustion and Flame* 117 (1-2) (1999) 4–31. doi:10.1016/S0010-2180(98)00071-6.  
URL <http://www.sciencedirect.com/science/article/pii/S0010218098000716>
- [14] M. H. Bordbar, G. Wecel, T. Hyppanen, A line by line based weighted sum of gray gases model for inhomogeneous CO<sub>2</sub>-H<sub>2</sub>O mixture in oxy-fired combustion, *Combustion and Flame* 161 (9) (2014) 2435–2445. doi:10.1016/j.combustflame.2014.03.013.
- [15] H. Bordbar, G. C. Fraga, S. Hostikka, An extended weighted-sum-of-gray-gases model to account for all CO<sub>2</sub>-H<sub>2</sub>O molar fraction ratios in thermal radiation, *International Communications in Heat and Mass Transfer* 110 (2020) 104400. doi:10.1016/j.icheatmasstransfer.2019.104400.  
URL <http://www.sciencedirect.com/science/article/pii/S0735193319302660>

- [16] V. P. Solovjov, F. André, D. Lemonnier, B. W. Webb, The Generalized SLW Model, *Journal of Physics: Conference Series* 676 (2016) 1–36.
- [17] V. P. Solovjov, F. André, D. Lemonnier, B. W. Webb, The rank correlated SLW model of gas radiation in non-uniform media, *Journal of Quantitative Spectroscopy & Radiative Transfer* 197 (2017) 26–44. doi:10.1016/j.jqsrt.2017.01.034.
- [18] J. Badger, B. W. Webb, V. P. Solovjov, An exploration of advanced SLW modeling approaches in comprehensive combustion predictions, *Combustion Science and Technology* 012022 (676) (2019) 1–17. doi:10.1080/00102202.2019.1678907.
- [19] P. J. Coelho, Radiative Transfer in Combustion Systems, in: F. A. Kulacki (Ed.), *Handbook of Thermal Science and Engineering*, Springer International Publishing, Cham, 2017, pp. 1–27. doi:10.1007/978-3-319-32003-8\_61-1.  
URL [https://link-springer-com.erl.lib.byu.edu/referenceworkentry/10.1007/978-3-319-32003-8\\_61-1](https://link-springer-com.erl.lib.byu.edu/referenceworkentry/10.1007/978-3-319-32003-8_61-1)
- [20] K. McGrattan, R. McDermott, C. Weinschenk, G. Forney, Fire dynamics simulator, technical reference guide, sixth edition (2013-11-04 2013). doi:https://doi.org/10.6028/NIST.sp.1018.
- [21] V. P. Solovjov, B. W. Webb, An Efficient Method for Modeling Radiative Transfer in Multicomponent Gas Mixtures With Soot, *Transactions of the ASME* 123 (2001) 450–457.
- [22] V. P. Solovjov, B. W. Webb, An Efficient Method for Modeling Radiative Transfer in Multicomponent Gas Mixtures With Soot, *Journal of Heat Transfer* 123 (3) (2001) 450–457. doi:10.1115/1.1350824.
- [23] V. P. Solovjov, D. Lemonnier, B. W. Webb, The SLW-1 model for efficient prediction of radiative transfer in high temperature gases, *Journal of Quantitative Spectroscopy and Radiative Transfer* 112 (7) (2011) 1205–1212. doi:10.1016/j.jqsrt.2010.08.009.
- [24] V. P. Solovjov, B. W. Webb, F. André, D. Lemonnier, Locally correlated SLW model for prediction of gas radiation in non-uniform media and its relationship to other global methods, *Journal of Quan-*

- titative Spectroscopy & Radiative Transfer 245 (2020) 106857. doi:10.1016/j.jqsrt.2020.106857.
- [25] V. P. Solovjov, B. W. Webb, SLW modeling of radiative transfer in multicomponent gas mixtures, *Journal of Quantitative Spectroscopy and Radiative Transfer* 65 (2000) 655–672.
- [26] V. P. Solovjov, B. W. Webb, Multilayer modeling of radiative transfer by SLW and CW methods in non-isothermal gaseous medium, *Journal of Quantitative Spectroscopy and Radiative Transfer* 109 (2) (2008) 245–257. doi:10.1016/j.jqsrt.2007.08.015.
- [27] V. P. Solovjov, D. Lemonnier, B. W. Webb, Extension of the exact SLW model to non-isothermal gaseous media, *Journal of Quantitative Spectroscopy and Radiative Transfer* 143 (2014) 83–91. doi:10.1016/j.jqsrt.2013.10.008.
- [28] B. W. Webb, V. P. Solovjov, F. André, An exploration of the influence of spectral model parameters on the accuracy of the rank correlated SLW model, *Journal of Quantitative Spectroscopy and Radiative Transfer* 218 (2018) 161–170. doi:10.1016/j.jqsrt.2018.06.023.
- [29] J. T. Pearson, B. W. Webb, V. P. Solovjov, J. Ma, Efficient representation of the absorption line blackbody distribution function for H<sub>2</sub>O, CO<sub>2</sub>, and CO at variable temperature, mole fraction, and total pressure, *Journal of Quantitative Spectroscopy & Radiative Transfer* 138 (2014) 82–96. doi:10.1016/j.jqsrt.2014.01.019.
- [30] V. P. Solovjov, J. T. Pearson, ALBDF: Absorption Line Blackbody Distribution Function (2014).  
URL <https://albdf.byu.edu/>
- [31] M. Q. Brewster, *Thermal Radiative Transfer and Properties*, 1992.
- [32] S. C. Lee, C. L. Tien, Optical constants of soot in hydrocarbon flames, *Symposium (International) on Combustion* 18 (1) (1981) 1159–1166. doi:10.1016/S0082-0784(81)80120-8.
- [33] V. R. Stull, G. N. Plass, Emissivity of Dispersed Carbon Particles, *Journal of the Optical Society of America* 50 (2) (1960) 121. doi:10.1364/JOSA.50.000121.

- [34] W. H. Dalzell, A. F. Sarofim, Optical Constants of Soot and Their Application to Heat-Flux Calculations, *Journal of Heat Transfer* 91 (1) (1969) 100–104. doi:10.1115/1.3580063.
- [35] C. R. Howarth, P. J. Foster, M. W. Thring (Eds.), *The Effect of Temperature on the Extinction of Radiation By Soot Particles*, Begellhouse, 1966. doi:10.1615/IHTC3.1210.
- [36] H.-c. Chang, T. T. Charalampopoulos, Determination of the wavelength dependence of refractive indices of flame soot, *Proceedings of the Royal Society of London. Series A: Mathematical and Physical Sciences* 430 (1880) (1990) 577–591. doi:10.1098/rspa.1990.0107.
- [37] J. D. Felske, T. T. Charalampopoulos, H. S. Hura, Determination of the Refractive Indices of Soot Particles from the Reflectivities of Compressed Soot Pellets, *Combustion Science and Technology* 37 (5-6) (1984) 263–283. doi:10.1080/00102208408923757.
- [38] T. C. Williams, C. R. Shaddix, K. A. Jensen, J. M. Suo-Anttila, Measurement of the dimensionless extinction coefficient of soot within laminar diffusion flames, *International Journal of Heat and Mass Transfer* 50 (7-8) (2007) 1616–1630. doi:10.1016/j.ijheatmasstransfer.2006.08.024.
- [39] J. D. Felske, C. L. Tien, The Use of the Milne-Eddington Absorption Coefficient for Radiative Heat Transfer in Combustion Systems, *Journal of Heat Transfer* 99 (3) (1977) 458–465. doi:10.1115/1.3450718.
- [40] H. Bordbar, personal communication RE: WSGG model implementation.
- [41] S. L. Chang, K. T. Rhee, Blackbody radiation functions, *International Communications in Heat and Mass Transfer* 11 (5) (1984) 451–455. doi:10.1016/0735-1933(84)90051-4.